Carbon monoxide line emission as a CMB foreground

Claudia G. Scóccola

Max Planck Institute for Astrophysics – Garching, Germany.

Talk based on 2 papers:

- Righi M., Hernández-Monteagudo, C. and Sunyaev, R. A&A 489, 489-504 (2008).
- Scóccola C., Hernández-Monteagudo, C. and Sunyaev, R. (in prep.).

Motivation

- The same star-forming activity that causes reionization of the IGM at $z \sim 10$ leaves an imprint on the CMB by means of several mechanisms, e.g.
  - Thomson scattering on the ionized gas,
  - resonant scattering on metals produced by the first stars,
  - IR emission from dust particles that reprocess UV radiation,

- In this talk, I will refer to the impact that emission on CO rotational lines have on the angular power spectrum of the CMB.

First stars:
production of C & O $\Rightarrow$ CO molecules — rotational transitions
CO($J = 1 \rightarrow 0$) $\nu = 115.3$ GHz

This line is very bright in:

- ∗ molecular clouds in our Galaxy (Wright et al. 1991; Fixsen et al. 1999)
- ∗ nearby star-forming galaxies (Weiss et al. 2005; Bayet et al. 2006; Baan et al. 2008)
- ∗ most distant quasars and radiogalaxies (Greve et al. 2005)

Lines emitted during the enhanced star formation epoch:
redshifted to CMB experiments frequency channels.

$\Rightarrow$ **CO is a foreground of CMB:** Contribution to the CMB power spectrum by the emission in such lines in *merging star-forming galaxies*.

Idea: To compute the angular power spectrum of the foreground fluctuations due to the emission in CO lines from merging star-forming galaxies.

Main difficulty: Presence of the continuum emission of dust at the same frequencies.

Proposal to separate the line contribution: To observe in several spectral bands with resolutions in the range $\frac{\Delta\nu}{\nu_{\rm obs}} = 10^{-1} - 10^{-3}$.

With this *varying spectral resolution* technique:

- The CO line signal increases (by 1 order of magnitude).
- Other foregrounds (continuum emission) remain unchanged.

Theoretical estimation of $C_\ell^{\rm CO}$'s:

Two main ingredients:

1. Model for the distribution of merging halos as a function of SFR:
    - Mass function:
        - Press-Schechter,
        - Sheth and Tormen,
        - Jenkins et al. (2001) (fit to numerical simulations)
    - Merger rate: Lacey and Cole formalism (Merging mass ratios: (0.1-10)).
    - Model for the star formation in each merging episode.
2. A relation (calibration) between the intensity of the line, and the star formation rate of the object.
   $L_{\rm CO\ line} = R\,\dot{M} \Rightarrow$ calibration using M82.

C_ℓ's due to emission by merging haloes has two terms:

* a correlation term that follows the underlying distribution of matter
* and a term that accounts for the Poisson fluctuations in the number counts

These are calculated in the *line of sight approach*, and the contributions come from Δz ($\frac{\Delta z}{z} \sim \frac{\Delta\nu_{\rm instr}}{\nu_{\rm obs}}$).

$$C_\ell^{\rm P} = \left[r^2 \frac{(\Delta\nu)_{\rm instr}}{\nu_{\rm obs}}\right]^{-1} \int dL_{\nu'(1+z)} cH^{-1}(z) \left(\frac{\tilde{L}_{\nu'(1+z)}}{4\pi}\right)^2 \frac{d\tilde{n}}{dL_{\nu'(1+z)}}$$

$$C_\ell^{\rm C} = \frac{2}{\pi} \int k^2 dk P_\psi(k) |\Delta_\ell(k)|^2 \qquad \text{with} \qquad \Delta_\ell(k) = \int dr j_\ell(kr) \mathcal{P}(r) [S(r)\delta_k]$$

where

$$S(r) \equiv \int dL_{\nu'(1+z)} dM G(M, L_{\nu'(1+z)}) \frac{dn}{dM} \frac{\tilde{L}_{\nu'(1+z)}}{4\pi} cH^{-1}(z) b(M, z[r])$$

Correlation and *Poisson* signals, for different $\left(\frac{\Delta\nu}{\nu_{\rm obs}}\right)$'s.

* Poisson fluctuations contribute down to much smaller scales (typical source size) and for them, further improvements on $\Delta\nu/\nu$ result in a larger amount of measured anisotropy.
* However, the actual amplitude of the Poisson term strongly depends on the ability of the observing instruments to isolate and remove the bright individual sources.

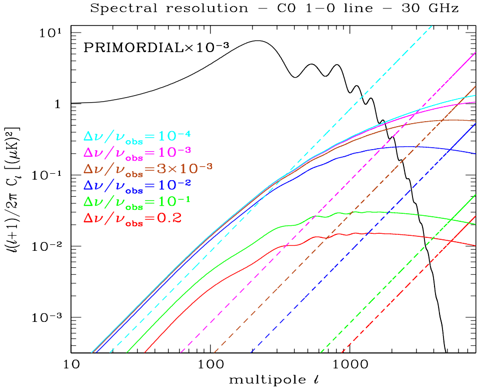

Dependence of the amplitude of the correlation signal on the spectral resolution.

* If sources are Poisson distributed, any improvement in the spectral/angular resolution of the experiment, will yield an increase in the measured power.

* However, sources are clustered in regions of $L_c \sim 15 - 25h^{-1}$ Mpc. The distribution of these regions will introduce more anisotropy, but only on scales that are larger than L_c (further improvement $\Rightarrow$ no diference).

* $\tilde{s}_i = \alpha f(\frac{(\Delta\nu)_i}{\nu}) + C + N_i$

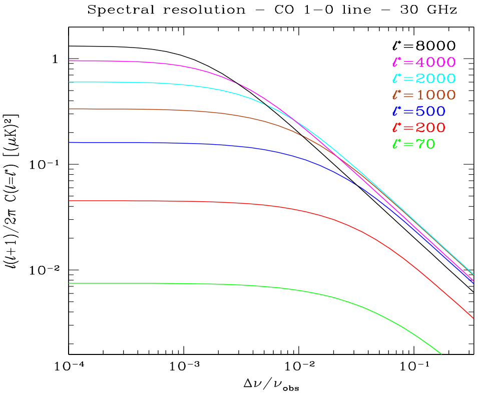

$$\Delta r = \frac{cH_0^{-1}}{\sqrt{\Omega_m(1+z)^3+\Omega_\Lambda}}\frac{\Delta\nu}{\nu_{obs}}$$

C_ℓ's for different mass functions:

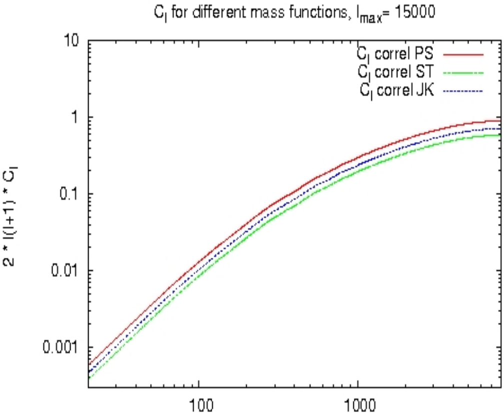

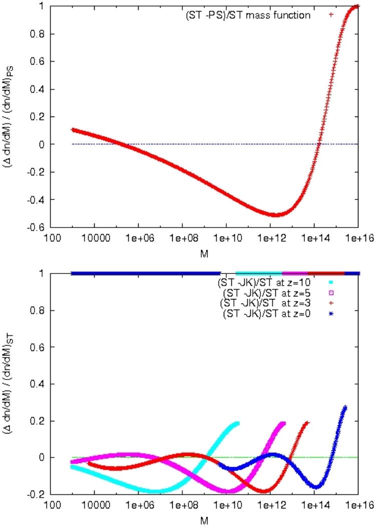

- $C_\ell^{ST} \sim 35\%$ lower than C_ℓ^{PS}
- $C_\ell^{JK} \sim 20\%$ lower than C_ℓ^{PS}

Conclusions

- Effect of the emission in CO lines particularly strong in the $20 - 60$ GHz frequency range.
- **Advantage:** Each observing frequency probes a given redshift shell ($\Delta z/z \sim \Delta\nu/\nu_{obs}$).
- The anisotropy will be optimally measured if both the angular and the spectral resolutions are able to spatially resolve the scales corresponding to the clustering.
- All the other foregrounds signals remain constant when varying the spectral resolution $\Rightarrow$ disentangle $\Rightarrow$ Tomography of reionization at different frequency bands.
- The emission on CO provides a new window into reionization, complementing the low-frequency observations pursuing the HI 21 cm fluctuations in the radio range.